

X-DIA DEMONSTRATOR AEROELASTIC TEST

J. Maleček*

Summary: *The work described in this contribution was performed as a part of the 3AS project (Active Aeroelastic Aircraft Structures) which is funded under contract (Contract No. G4RD-CT-2002-00679) of the European Union. The paper deals with the tests of the X-DIA component aeroelastic demonstrator (the front part of the fuselage with the foreplane of the three plane jet transport aircraft) in the VZLU Prague.*

1. Introduction

The VZLÚ Aeroelasticity Group has been collaborated in the Fifth FP EC Project "Active Aeroelastic Aircraft Structures (3AS)" during the 2002 – 2005 years. The main object of this project was to employ aeroelastic behaviour of the aircraft structure to increase its operational efficiency. A number of concepts and procedures was investigated and verified on some demonstrators. The concept "Active All-Movable Foreplane (AAMFP)" incorporated in the work package "Active Aeroelastic Concepts based on Adaptive Attachment/Stiffness" was validated by means of the X-DIA demonstrator. The main aim of the solved task was to develop and verify the active control vibration system with using of the foreplane. The X-DIA demonstrator was adapted from the older remote controlled vehicle – see fig. 1, which was developed in the Politecnico di Milano.

Three institutions have been shared on the verifying of the AAMFP concept. The front part of the new fuselage, the electric foreplane drive, the hardware and software of the active



Fig. 1 Original X-DIA demonstrator

* Ing. Jaromír Maleček, CSc.: Výzkumný a zkušební letecký ústav (VZLÚ), a.s.; Beranových 130; 199 05 Praha 9 – Letňany; tel.: +420.225 115 123, fax: +420.283 920 018; e-mail: malecek@vzlu.cz

control device, the assembly of the demonstrator and the debugging of the A/C system were performed in the PoliMi. The task definitions and requirements, the numerical analysis, concepts of the design, the design, manufacture and verifying of the forward swept foreplane were worked up in the DLR Göttingen. The analyses of the demonstrator, design and manufacture of the special wind tunnel attachment and the backward swept foreplane; stiffness test, modal and wind tunnel ones and the assessment of results were performed in the VZLÚ. The experimental validation was divided into two parts. The X-DIA component demonstrator was tested in the VZLÚ Ø 3 m low speed wind tunnel (from May to June 2004), the X-DIA complete demonstrator was tested in the PoliMi 4x4 m wind tunnel.

2. Test aim formulation

The main test objective of the X-DIA demonstrator of the component model of the front part of the fuselage with two variants of foreplanes (abbreviated as the X-DIA demonstrator or demonstrator only) was to gain basic parameters serving for the analytical models improving and to verify the active control device for the fuselage vibration suppression.

Firstly the measurement of mass, stiffness and modal parameters of the X-DIA demonstrator was planned. The investigation of the static aerodynamic characteristics – aerodynamic coefficients, structure loads, structure deformations – was demanded in the first phase of the wind tunnel test. The verification of the active control device effectiveness at the dynamic structure response to the external excitation was planned.

3. Demonstrator description

The X-DIA demonstrator (see fig. 4) is a one-dimensional sectional concept. The fuselage stiffness has been simulated by the duralumin box beam. The fuselage aerodynamic and mass parameters have been realised by ten body sections manufactured from carbon composites.

The foreplanes with backward sweep (sweep angle $\chi = 25^\circ$, span $l = 1.414$ m, VZLÚ model A) and with forward one ($\chi = -25^\circ$, $l = 1.3$ m, DLR model B) were manufactured from carbon box beam, sandwich ribs and the stressed carbon skin. Both halves of the foreplane have been connected to the drive device by metal pivots.

The X-DIA demonstrator has been equipped with an electric drive of both foreplane halves independently – see fig. 5. The drive makes possible the foreplane angle declinations $\delta = \pm 12.5^\circ$ (symmetric, antisymmetric, static, harmonic with constant or swept frequency). The drive control works up to 25 Hz. The software of the active control device makes possible to elect various values of the gain and to switch off it (gain 0).

4. Stiffness test

The X-DIA demonstrator with a fuselage beam cantilevered to a stiff framework was loaded by horizontal and vertical forces by means weights in the fuselage nose and by symmetric and antisymmetric forces and couple of forces in tips of both foreplane variants. A typical arrangement of the stiffness test is perceptible in fig. 2, the backward swept foreplane is loaded by an antisymmetric torsion moments. The torsion load of foreplanes was introduced either at a mechanical or at an electrical blocked drive. The deflection was scanned by

incremental indicators in 33 points. The gained results were worked up in the form of the compliance influence coefficients matrix.

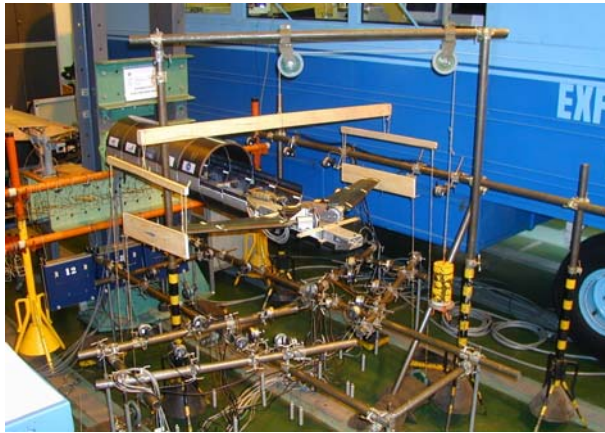


Fig. 2 Stiffness test arrangement



Fig. 3 Ground vibration test arrangement

5. Ground vibration test

The aim of the X-DIA demonstrator ground vibration test (GVT) was to identify modal parameters of two demonstrator variants with back/forward swept foreplanes. The GVT results were used for a tuning of a dynamic analytical model, as an input for an analytical verification of dynamic aeroelastic behaviour and as basic information for an interpretation of wind tunnel investigations results.

The fuselage beam was connected to a massive supporting framework during the GVT. The test was performed with mechanical blocked foreplanes.

The used PRODERA test facility contains the circuits for excitation, measuring, carrying out analysis of vibration and for a test control. The demonstrator was excited by three electrodynamic shakers with 50 N maximal forces. The vibrations were measured by means of accelerometers in 39 points.

The distribution of natural frequencies of the demonstrator was determined up to 60 Hz using the analysis of responses upon the sine excitation. Modal parameters (natural frequency, generalised mass, damping ratio and mode shape) of individual modes were obtained by means of a complex power method. The measured natural frequencies of two demonstrator variants are introduced in the tab. 1. The red high-lighted modes were suppressed at the wind tunnel test.

Tab. 1 Ground vibration test - natural frequencies

Mode	Model A (VZLU FP)	Model B (DLR FP)
	f [Hz]	f [Hz]
1st vertical fuselage bending	3.841	3.689
1 st horizontal fuselage bending	5.158	4.967
1st fuselage torsion	21.65	19.10
2 nd vertical fuselage bending	31.65	31.49
2 nd horizont. fuselage bending	35.81	38.04
1 st vert. sym. foreplane bend.	39.27	52.62

6. Wind tunnel test

6.1 Test arrangement

Attachment of the X-DIA demonstrator. The X-DIA demonstrator with/without foreplanes was tested in the wind tunnel – see fig. 4. With respect to the relative high value of the natural frequency of the fuselage torsion mode the attachment was analysed and optimised to the



Fig. 4 Wind tunnel test arrangement



Fig. 5 Detail of the foreplane drive system

needed stiffness. The strain-gauges aerodynamic balance (between the support and the fuselage beam) used for the static test was relatively flexible and was replaced by the stiff element at the dynamic test.

Wind tunnel. The VZLU low-speed wind tunnel is circulating one with the open test area with the \varnothing 3 m circular cross-section and the 3 m length. The maximal flow velocity is 70 ms^{-1} . There was installed a protective net behind the model. The relatively big demonstrator was in the whole range of the angle of attack adjustment situated in the flow core with the constant velocity profile and known turbulence spectral parameters.

6.2 Procedure of the test process

Testing facilities. Quantities characterizing aerodynamic forces and moments, model structure load and model deformations were investigated at the static test.

Aerodynamic forces and moments were scanned by the six-component strain-gauge aerodynamic balance. Loads of the demonstrator were sensed by strain gauges placed on the fuselage beam (bending moment, torsion moment). Pitch and roll angular deformations of the demonstrator were detected by inclinometers in two sections of the fuselage.

Bending deformations of the model at the static test were scanned by contactless optical sensors along the foreplane span in 25% of the chord and on the fuselage. Translations in the vertical direction were evaluated from the shift of a video record of the laser mark generated by sensors.

For evaluation of responses at the dynamic test, the signals from strain gauges, inclinometers and accelerometers were used. Signals sampled with 200 Hz frequency were processed by the LabVIEW system.

The external excitation of the model was realized by the hydraulic cylinder through the string with the rubber spring eccentrically to the left side of the sixth fuselage body section – see fig.4. The exciting force and the translation were scanned by the impedance head.

Because of the active control demands seven accelerometers were installed on the structure. The active control system has worked under a PC running the real time operating system known as RTAI – Linux, developed at Aerospace Eng. Department of PoliMi. This control system features an application of a PID regulator and the implementation of the ILAF (Identical Location of Aerodynamic Force) control system.

Both halves of the foreplane are driven by electro motors separately – see fig. 5. The system makes possible to adjust the symmetric or anti symmetric static deviations in the range of $\pm 12.5^\circ$ (stoppers) and to vibrate. The active control SW makes possible to define different values of the gain and switch on/off this device.

The PC used for the data acquisition and for the generating of the external excitation was equipped with the NI 6034 E and NI 6036 E acquisition cards.

Test process. At the static wind tunnel test of the X-DIA demonstrator in the attachment arrangement with the aerodynamic balance the tested points were investigated for the selected model variant and selected foreplane deviation δ at automatically changed angle of attack α .

At the dynamic wind tunnel test the X-DIA demonstrator was excited by external shaker firstly at the speed $V = 0$ m/s and then at the selected speed levels with the active control system off (gain = 0) or on (selected values of gain) by the frequency linear sweep input.

Evaluation of test results

Static test. Signal components of the aerodynamic strain-gauge balance were processed into the coefficients c_D , c_L , c_Y , m_x , m_y , m_z (drag, lift, side force, roll, pitch, yaw moment coefficients, resp.). The drag coefficient c_D with regard to small values of the used Re number could be used only for the comparison of model variants and the transformation to the full-scale structure is questionable.

From the tested dependences of the aerodynamic coefficients c_L , m_y , m_x the derivatives c_L^α , c_L^δ , m_x^δ , m_z^α , m_y^δ were computed.

Demonstrator structure loads – bending and torsion moment on the fuselage beam – were monitored on line at the static test. From the static stiffness test, the admissible ranges of the loads and deformations were determined. After the exceeding of the load envelope the test was interrupted.

Demonstrator angle deformations from inclinometers (pitch, roll) and contactless optical indicators were worked up in dependences on the flow speed and model parameters.

Dynamic test. Transfer functions of the output signals from strain gauges, accelerometers and inclinometers and the input signal (exciting force in the impedance head) were computed. The spectra were arranged into the form, which enables to assess the dynamic effectiveness of the A/C system.

6.3 Wind tunnel test results

Static test

Review of static test points

Static tests were performed on the three basic X-DIA demonstrator configurations: the front part of the fuselage equipped with two variants of the foreplanes (backward/forward sweep)

and without one. Following parameters were changed: the fuselage angle of attack α , the symmetric/anti symmetric foreplane deflection δ and the flow speed V .

Aerodynamic coefficients

The selected main measured dependences of the lift coefficient c_L (example see fig.7), pitching moment coefficient m_y (c_{me2}) (fig. 6), rolling moment coefficient m_x (c_{le2}) (fig.8) in dependence on the angle of attack α , for parameters of foreplane deviations δ , flow speed V and three demonstrator variants (back/forward swept FP, without FP) were assessed.

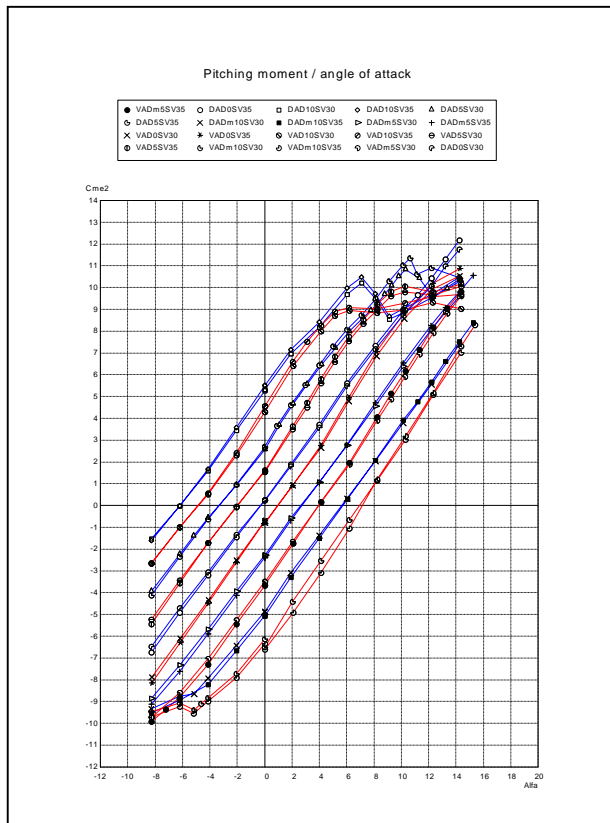


Fig. 6 Pitching moment coefficient m_y versus angle of attack α
FP variant: **back/forward** sweep,
symmetric $\delta = 0^\circ, \pm 5^\circ, \pm 10^\circ$

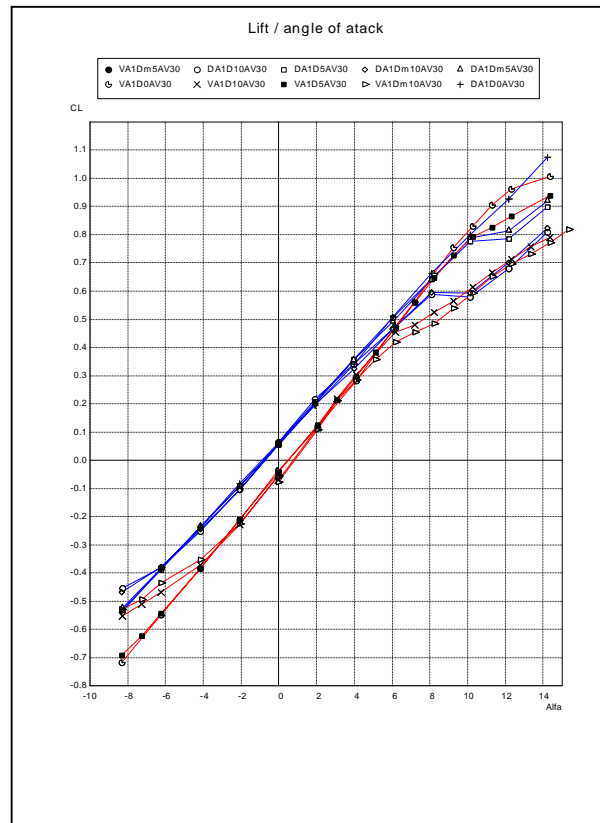


Fig. 7 Lift coefficient c_L versus angle of attack α
FP variant: **back/forward** sweep,
antisymmetric $\delta = 0^\circ, \pm 5^\circ, \pm 10^\circ$

We remind the aerodynamic section body model with slots and unevenness of its shape isn't too proper for the correct test of aerodynamic coefficients at higher values of α . Especially measured values of the drag coefficient c_D with regards to effected low values of the Re number aren't reliably transformable to the full scale structure. Presented tested dependences can be used to the direct comparison both main model variants with back/forward swept foreplanes – see fig. 9.

The functions of the lift effectiveness c_L^α and c_L^δ , the effectiveness in the pitch m_y^α and m_y^δ and the effectiveness in the roll m_x^δ were computed from coefficients.

The effectiveness of c_L^α , c_L^δ , m_y^α , m_y^δ for symmetric angle of incidence δ and m_x^δ for antisymmetric δ in dependence on the speed for both foreplane variants were worked up.

The values have corresponded to the linear part of the aerodynamic coefficients dependences. The backward swept foreplane effectiveness is higher than the effectiveness of the forward swept one. The effectiveness is gentle growing.

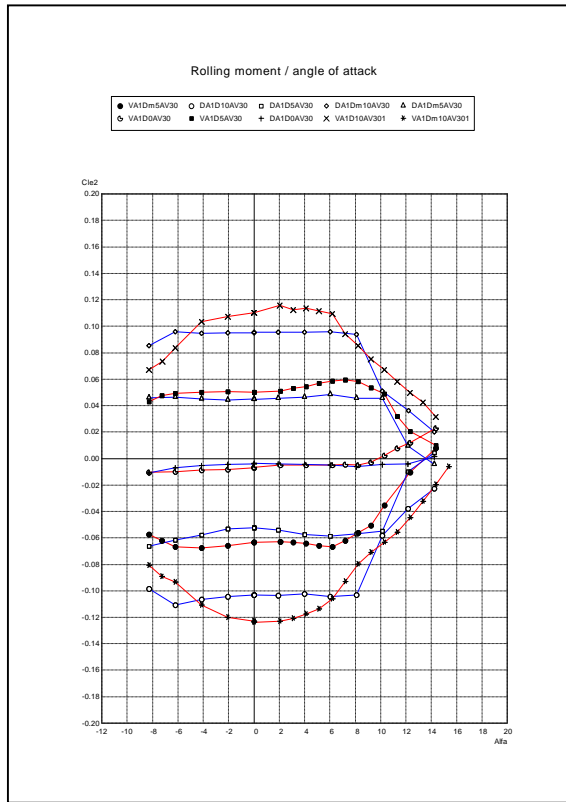


Fig. 8 Rolling moment coefficient m_x versus angle of attack α
 FP variant: **back**/**forward** sweep,
 $V = 30$ m/s,
 antisymmetric $\delta = 0^\circ, \pm 5^\circ, \pm 10^\circ$

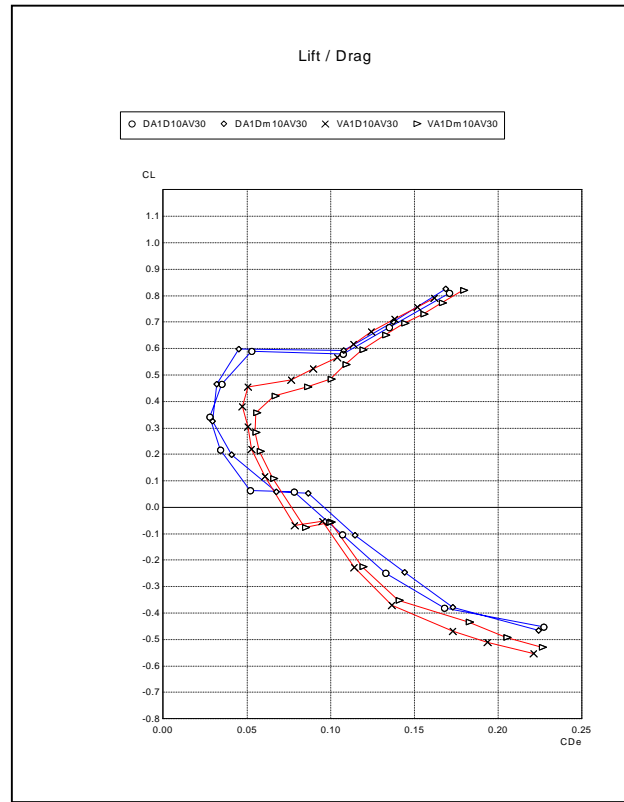


Fig. 9 Polar diagram
 FP variant: **back**/**forward** sweep,
 $V = 30$ m/s,
 antisymmetric $\delta = \pm 10^\circ$

Model structure loads

There is the bending moment M_y and torsional moment M_x indicated by strain gauges on the fuselage beam in fig. 10 and 11.

The data of loads were monitored on-line; the permissible load envelope was used for the permanent checking of the model structure safety at the wind tunnel test. The envelope was determined at the demonstrator stiffness test.

Model structure deformations

There is the deformation of the forward swept foreplane spanwise in five points of the rotation axes measured by the optical contactless system in fig. 12. The twisting of the demonstrator in the point of the foreplane attachment is roughly 0.5° . The deformation distribution shows on the change of the stiffness in the cantilevering point of the foreplane halves.

There are the roll and pitching deformations for the model variants equipped with the back/forward swept foreplanes in the dependence on the speed and various values of the α

and δ in the fig. 18 and 19. The angle deformations were measured in two fuselage beam sections (half, tip). The deformation of the model variant with the forward swept foreplane is higher with regard to the acting arm.

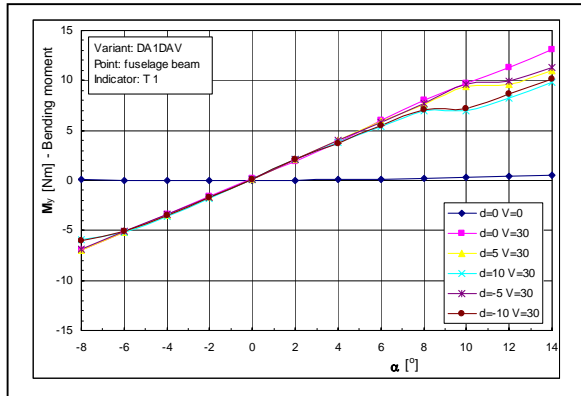


Fig. 10 Load of the structure – bending moment
FP variant: forward sweep, $V = 0, 30$ m/s
antisymmetric $\delta = 0^\circ, \pm 5^\circ, \pm 10^\circ$

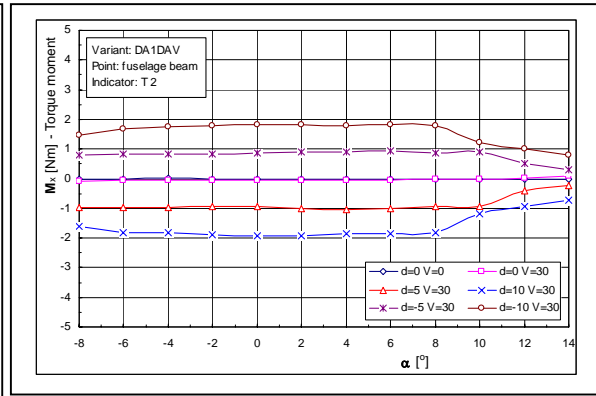


Fig. 11 Load of the structure – torque moment
FP variant: forward sweep, $V = 0, 30$ m/s
antisymmetric $\delta = 0^\circ, \pm 5^\circ, \pm 10^\circ$

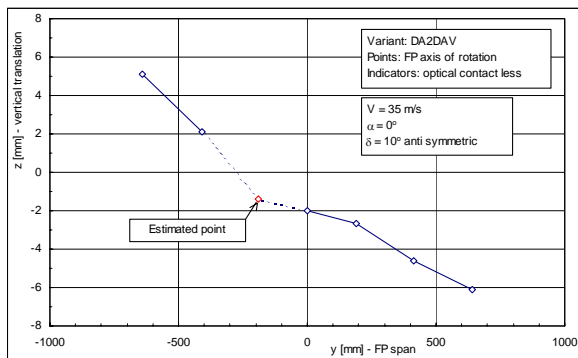


Fig. 12 Foreplane deformation
FP variant: forward sweep, $V = 35$ m/s,
anti symmetric $\delta = 10^\circ$

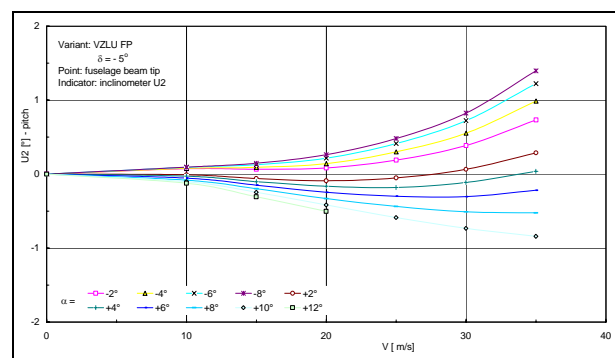


Fig. 13 Fuselage deformation
FP variant: backward sweep,
symmetric $\delta = - 5^\circ$

Dynamic test

Review of dynamic test points

Dynamic tests were performed on the basic X-DIA demonstrator configurations: the front part of the fuselage equipped with back/forward swept foreplanes.

The model was excited by the external shaker on the left side of the foreplane body. The A/C system can suppress the symmetric and the antisymmetric vibration modes separately or both types of modes simultaneously in the selected frequency ranges.

Active control tests

Firstly the transfer functions of six scanned outputs of the X-DIA demonstrator equipped with the back/forward swept foreplanes at $V = 0$ m/s were tested. The gained natural frequencies were compared with the GVT results.

The transfer functions z/F_z (z displacement integrated from \ddot{z}) (fig. 14a) and M_y/F_z of the model variant with the back/forward swept foreplanes concerning the active control of the symmetric vibration in the range of the 3.5 – 4.5 Hz and M_x/F_z (M_x – torsional moment) (fig. 14a) in the range of the torsional natural frequency at the A/C OFF and ON for various values of the gain and flow speeds were investigated.

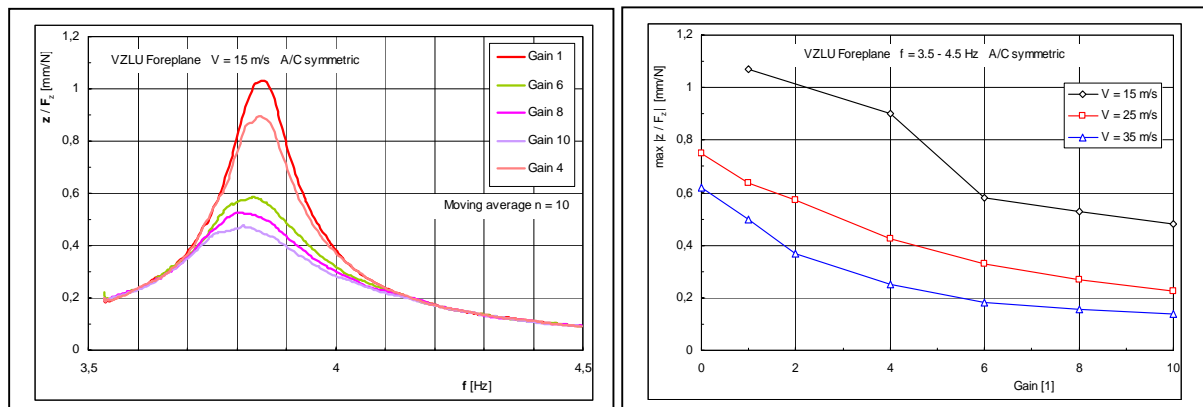


Fig.14 a, b Gain effectiveness

Transfer function: fuselage beam nose translation z / exciting force F_z ,
FP backward sweep, $V = 15$ m/s, A/C symmetric, $f = 3.5 - 4.5$ Hz

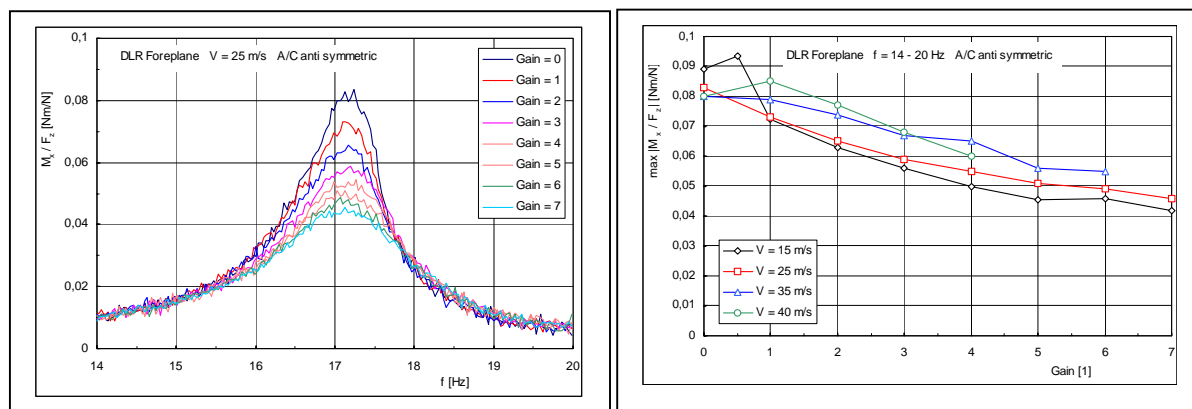


Fig.15 a, b Gain effectiveness

Transfer function: fuselage beam torsional moment M_x / exciting force F_z ,
FP forward sweep, $V = 25$ m/s, A/C anti symmetric, $f = 14 - 20$ Hz

The effectiveness of the A/C system at various gains and flow speeds is presented in fig. 14b (backward swept foreplane, symmetric bending) and in fig.15b (forward swept foreplane, torsion). The effectiveness has been rated accordingly to the value of the peak of the transfer function at the corresponding mode.

7. Conclusion

Two main variants of the X-DIA component model with the backward and forward sweep foreplanes were tested in the VZLÚ (stiffness test, ground vibration and wind tunnel ones).

The aerodynamic characteristic, model structure loads and deformations were performed at the static wind tunnel test. Static effectiveness in lift, pitching and rolling of the demonstrator equipped with backward swept foreplane have been higher than of the demonstrator with forward swept one and have been slightly growing with the speed increasing.

The tested aerodynamic characteristics have been influenced by the compliance of the foreplane drive, the low value of the Re number and the unevenness of the body shape in outer parts of the investigated range of the angle of attack α and the foreplane incidence δ . Tested dependences have fully satisfied the needs of the comparison of both demonstrator variants, but their transformation to the full-scale structure will be questionable.

The symmetric deformations of the demonstrator with the forward swept foreplane have been greater than one with the backward swept variant.

The effectiveness of the A/C system was confirmed at the dynamic wind tunnel test.

8. Acknowledgement

The paper deals with the VZLÚ contribution to the 5th FP EC Project “Active Aeroelastic Aircraft Structures (3AS)“, which was funded under contract of the European Union (Contract No. G4RD-CT-2002-00679). The presentation of the paper was approved by the “3AS” project partners and the EC representative.

This paper was prepared in the frame of the project “Strength Research of the Low-Weight Aircraft Structures“ (No. MSM 0001066903) funded from the Czech Ministry of Education.

9. References

- Kiessling, F. (2002) Contribution to Objectives and Requirements for an Active All-Movable Fore Plane (AAMFP) Concept, 3AS Report, Delivery D 4.3-1, Issue 1, 29.09.2002, Contract No. G4RD-CT-2002-00679, DLR Goettingen.
- Černý, O. & Hlavatý, V. (2004) Ground Vibration Test of the X-DIA front fuselage with foreplanes (mod. A and B) aeroelastic scaled model, 3AS Report, Deliverable D 4.3.6, Contract No. G4RD-CT-2002-00679, VZLÚ Prague.
- Čečrdle, J. & Maleček, J. (2004) New Foreplane for Active All-Movable Fore Plane (AAMFP) Concept, 3AS Report, Delivery D 4.3.2, Issue 1, Contract No. G4RD-CT-2002-00679, VZLÚ Prague.
- Ricci, S. & Scotti, A. & Zanotti, D. (2004) X-DIA Front-fuselage model Installation Instructions & Control System Software Manual (Ver.1.0 Xrtailab), Draft, Contract No. G4RD-CT-2002-00679, PoliMi.
- Maleček, J. (2004) Stiffness Test of the X-DIA Component Model, 3AS Project, Deliverable D 4.3.7, Contract No. G4RD-CT-2002-00679, Prague.
- Maleček, J. & Čečrdle, J. (2004) Wind Tunnel Test of the X-DIA Component Model, 3AS Project, Deliverable D 4.3.7, Contract No. G4RD-CT-2002-00679, Prague.